

SYNTHESIS AND CHARACTERIZATION OF THIOL - CAPPED SILVER NANOPARTICLES AND THEIR EFFECT ON LIQUID CRYSTALS

K. Sivaram¹, M.C. Rao², G. Giridhar³, M. Tejaswi¹, B.T.P. Madhav⁴,
V.G.K.M. Pisipati⁴ and R.K.N.R. Manepalli^{1*}

¹Department of Physics, The Hindu College, Krishna University, Machilipatnam-521001, India

²Department of Physics, Andhra Loyola College, Vijayawada-520008, India

³Department of Nanotechnology, Acharya Nagarjuna University, Guntur-522510, India

⁴LCRC-R&D, Department of ECE, K. L. University, Guntur-522502, India

*Email: manepalli.67@gmail.com

ABSTRACT

Synthesis and characterization of Liquid Crystalline p-n-decyloxy benzoic acid (10OBA) compound with thiol-capped Ag nanoparticle dispersion was carried out by chemical reduction method. The Polarizing Microscopy (POM), Differential Scanning Calorimeter (DSC) technique are used to measure the Glass transition temperature (T_g) and melting temperature (T_m) of the prepared samples. Spectroscopic techniques like X-ray Diffraction spectrometric studies (XRD), Scanning Electron Microscopic studies (SEM), Ultra-Violet Visible (UV) spectroscopy, Fourier Transform Infra Red Spectroscopy (FTIR) were also carried out on to the samples. Textural determinations of the synthesized compounds are recorded by using POM connected with a hot stage and camera. The results showed that the dispersion of thiol-capped Ag nanoparticles in 10OBA exhibited NC phases as that of the pure 10OBA with reduced clearing temperature as expected. The order parameter is estimated from birefringence anisotropy data without considering any internal field model to liquid crystal molecule and with dispersed thiol-capped Ag nanoparticles. It is found that the birefringence anisotropy as well as orientational order parameter of 10OBA increased with dispersed 1 wt% thiol-capped Ag nanoparticles.

Keywords: Synthesis, POM, DSC, Nanodispersion, XRD, SEM, UV spectroscopy, FTIR, Birefringence and Order parameter.

© RASAYAN. All rights reserved

INTRODUCTION

The electrical and optical properties of liquid crystal (LC) is mainly dependent upon the intrinsic characteristics, phase structure, molecular size, concentration of the nanoparticles (NPs) used for doping^{1,2}. A similar relation of characteristics is observed between the nanoparticles and LC molecules, the size of the molecules that would not significantly disrupt the order of the LC. On doping of NPs in LC host, it improves spontaneous polarization as well as vital physical properties and improves the electro-optical properties of the LC devices. After doping of nanoparticles in LC host, the anisotropic dielectric constant increases as a result threshold voltage is decreases in both electrically controlled birefringences. Now a day's much attention takes place towards the Liquid Crystals due to their anisotropy nature and enhances their mechanical, electrical and optical properties, which behaves like solid crystals.

As it has no ability to obtain shearing but flows like ordinary isotropic solutions (liquids) which have a tendency to transfer their long-range orientation order on the dispersed materials such as nanoparticles and various colloids³⁻⁵. A variety of applications has been taken place while the dispersion of metal nanoparticles into the moiety of LC. These nanodoping materials investigated include metallic nanoparticles, semiconducting nanoparticles, ferroelectric nanoparticles, carbon-related nanoparticles and other⁶⁻⁸.

The capping agent helps to prevent the uncontrollable growth of particles; prevent particle aggregation, control growth rate, and particle size⁹. In the present work thiol-capped Ag nanoparticles are

synthesized and dispersed into the p-n-decyloxy benzoic acid (10OBA). Silver nanoparticles have been widely utilized to exploit their novel properties (e.g. anti-bacterial properties, catalysis and bio-sensing) and their possible risks (e.g. toxicity and possible cancer risk) have been researched extensively¹⁰⁻¹⁵. Rao et al. have published their results on different oxide materials, luminescent materials and polymers in their earlier studies¹⁶⁻⁴². Silver nanoparticles have been dispersed in LC to obtain different types of compounds with different structures.⁴³

EXPERIMENTAL

Synthesis of thiol-capped Silver nanoparticles

Silver nano particles (AgNO_3) with proper weight of 150 mg are dissolved in 30 ml of distilled water and it is added to the solution of 225mg of Tetra Octyl Ammonium Bromide (TOAB) in 24 ml of toluene. The resultant solution is continuously stirred for 20 minutes, poured in dodecane thiol of 0.189ml of solution and the obtained homogeneous solution is stirred further for 10 minutes.

A proper weight of 398 mg of NaBH_4 dissolved in 24 ml of water is mixed with the above-obtained solution, after getting completely mixtures the solution is again stirred at room temperature (RT) about 3 hours. From The obtained solution the organic phase is separated and placed 2 to 3 ml of solution in arotary evaporator under vacuum at RT. The solution is mixed with 50 ml of ethanol and placed at 5000 rpm for 1 hour to get centrifuged. The supernatant (floating on the surface of the liquid) liquid is removed.

The resulting dodecane thiol protected Ag nanoparticles are completely dissolved in 1ml of dichloromethane to get precipitate which is washed with ethanol. The above re-dispersal process was repeated several times for complete removal of non-covalently bonded organic material. After the centrifugation process, 60 mg of thiol-capped Ag nanoparticles are obtained.

Dispersion of thiol-capped Ag nanoparticles in 10OBA

For uniform dispersion of nanoparticles into 10OBA, 1wt % of thiol-capped Ag nanoparticles are dissolved in toluene and completely stirred well about 1Hr to get the isotropic state of LC material (10OBA) and stirred well about three hours. After cooling, the phase transition temperature of nanocomposite 10OBA is analyzed by using Polarizing Optical Microscope (SDTECHS make) with a hot stage at which the obtained material was filled in a planar arrangement in 4 μm cells, along with the thermometer described by Gray⁴⁴.

The Textural, phase transition temperatures and enthalpy values of Ag nanoparticles were studied by Differential Scanning Calorimeter (Perkin Elmer Diamond DSC). Fourier transform Infrared (FTIR) is a versatile tool for identifying types of chemical bond in a molecule by producing an FTIR absorption spectrum.

X-ray diffraction technique is used to determine the grain size of the Ag nanoparticles which are dispersed in LC compounds. The presence of Ag nanoparticles in 10OBA is studied by SEM data. Modified Spectrometer is used to determine the birefringence anisotropy data of the LC molecules with the dispersion of 1wt% of thiol-capped Ag nanoparticles.

RESULTS AND DISCUSSION

Polarizing Optical Microscope

The transition temperatures and textures observed by Polarizing Microscope in pure 10OBA are shown in Fig.-1(a-c) while that of 10OBA with dispersed thiol-capped Ag nanoparticles with 1 wt% concentration shown in Fig.-2(a-c) respectively.

The thermal ranges of nematic and smectic C phases are changed slightly due to the dispersion of nanoparticles and the textures of the phase's changes by the self-assembly of nanoparticles. The DSC thermograms are shown in Fig.-3 and Fig.-4.

The transition temperatures and enthalpy changes at the phase transformations determined through POM and DSC. It is observed that the transition temperatures are lowered with the dispersion of thiol-capped Ag nanoparticles dispersed in 10OBA.

Textures of 10OBA PURE

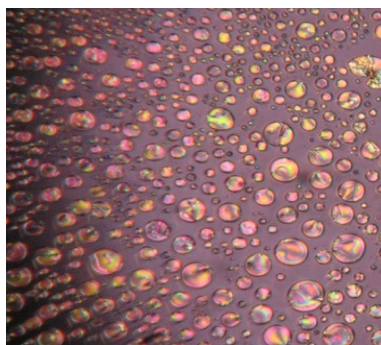


Fig.-1a: Smectic phase at 138.7 °C

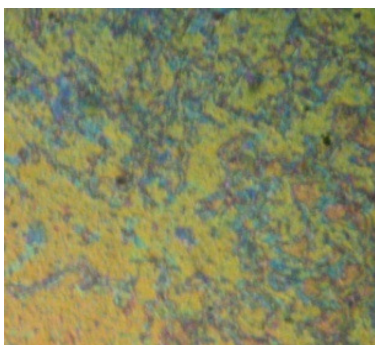


Fig.-1b: Smectic C phase at 119.9 °C

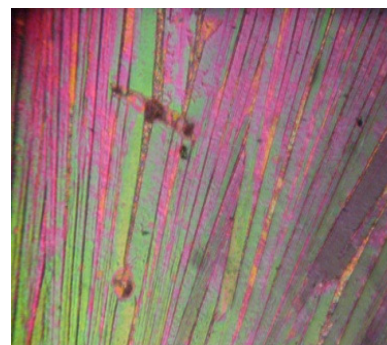


Fig.-1c: Solid phase at 91.5 °C

Textures of 10OBA+1% Ag nanoparticles



Fig.-2a: Nematic droplets 134.3 °C

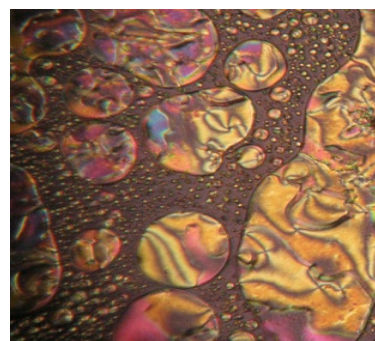


Fig.-2b: Schlieren nematic at 127.8 °C

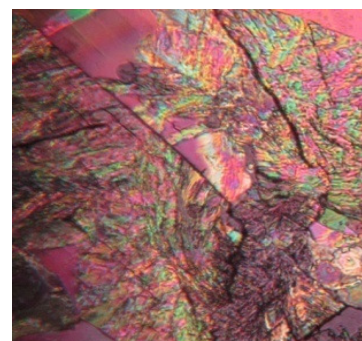


Fig.-2c: Solid at 90.4 °C

DSC Thermograms

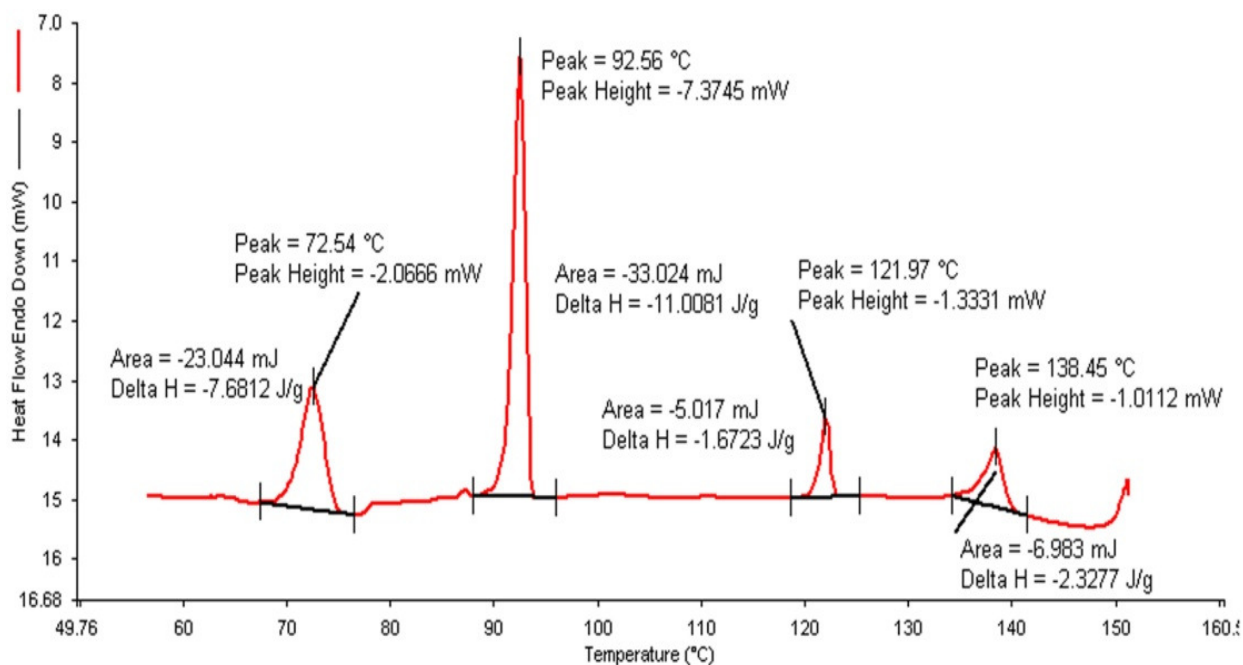


Fig.-3: DSC Thermogram of 10OBA pure compound

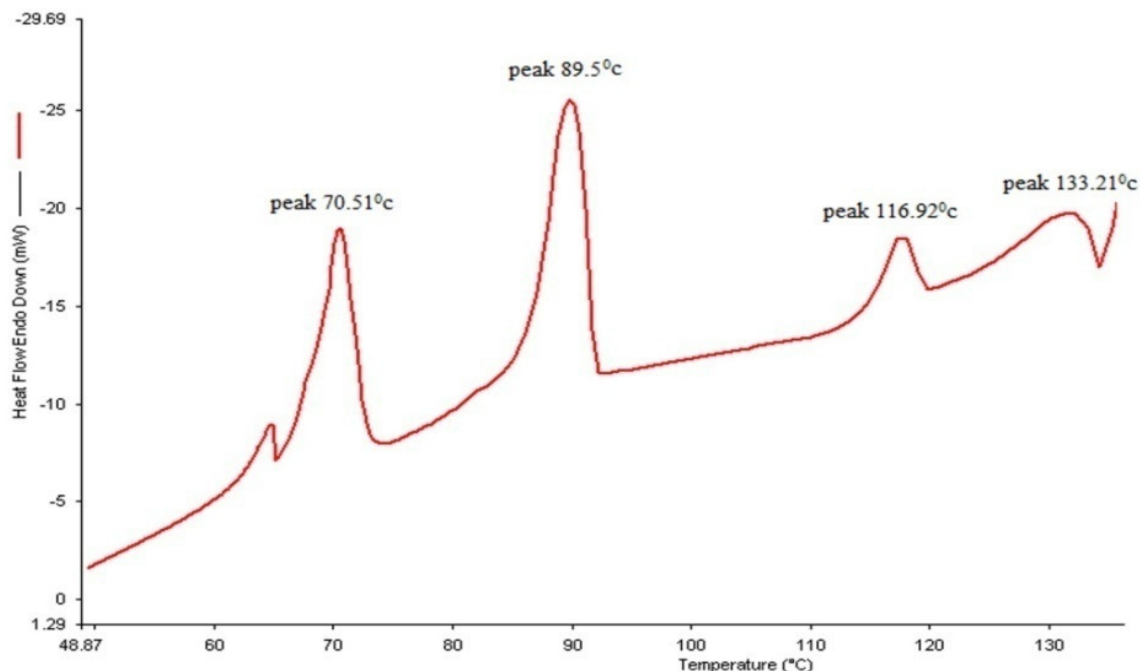


Fig.-4: DSC Thermogram of 10OBA with 1wt % thiol-capped Ag nanoparticles

Ultraviolet –Visible (UV) Spectroscopy

Fig.-5 shows the UV-visible spectra of pure and thiol-capped Ag nanoparticles doped in 10OBA LC sample. It is observed that the spectrum for pure 10OBA does not exhibit any absorption peaks in the wavelength range 400–500nm. However, the spectrum of nanodoped 10OBA shows the significant peak at 435nm, which are the characteristic peak of thiol-capped Ag nanoparticles. So, the UV-visible spectral study confirms the presence of thiol-capped Ag nanoparticles in the prepared nanodoped LC.

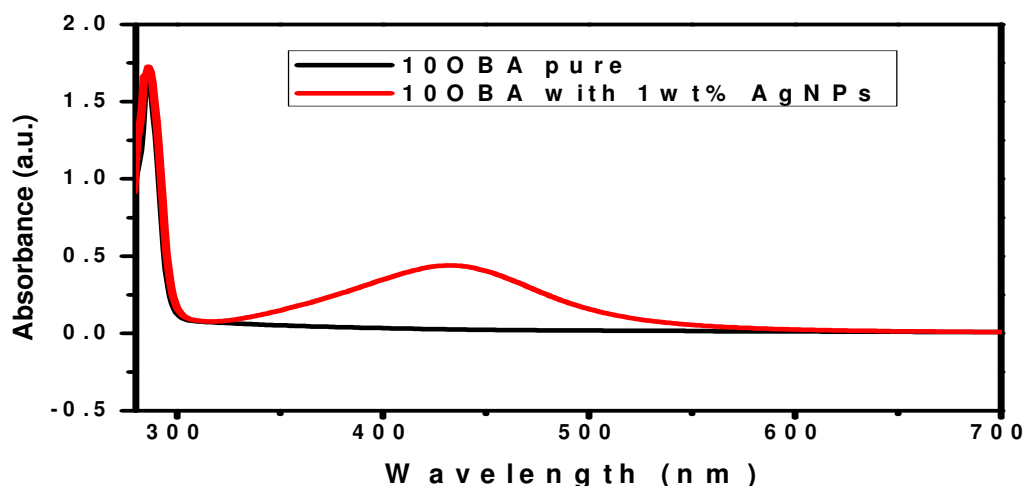


Fig.-5: UV-visible spectra of 10OBA with 1 wt % thiol-capped Ag nanoparticles

FTIR Analysis

The FTIR spectra of free dodecane thiol and particles capped by dodecane thiol are shown in Fig.-6 and Fig.-7. The peaks obtained at 723 cm^{-1} which correspond to the C-S stretching mode, the rocking mode

of the peak is obtained due to a terminal methyl group at 1027 cm^{-1} , where as non-rocking mode of the peak is obtained due to a methyl group at 1271.45 cm^{-1} and wagging mode occurring at 1467 cm^{-1} . The stretching modes of the terminal methyl groups, occurring in the range 2800 to 3000 cm^{-1} . The stretching mode of C-S bond forms due to its existence of a chemical bond between S ions and Ag ions. On comparison FTIR spectra of dodecane thiol with thiol-capped silver spectra reveals the same existency of peaks, but the intensities of peaks at different frequencies change due to Ag nanoparticles^{45,46}. A qualitative explanation of FTIR spectra reveals that alkanethiol molecules adsorbed on the Ag nanoparticle surfaces and dodecanethiol play a key role in the formation of composite nanoparticles.

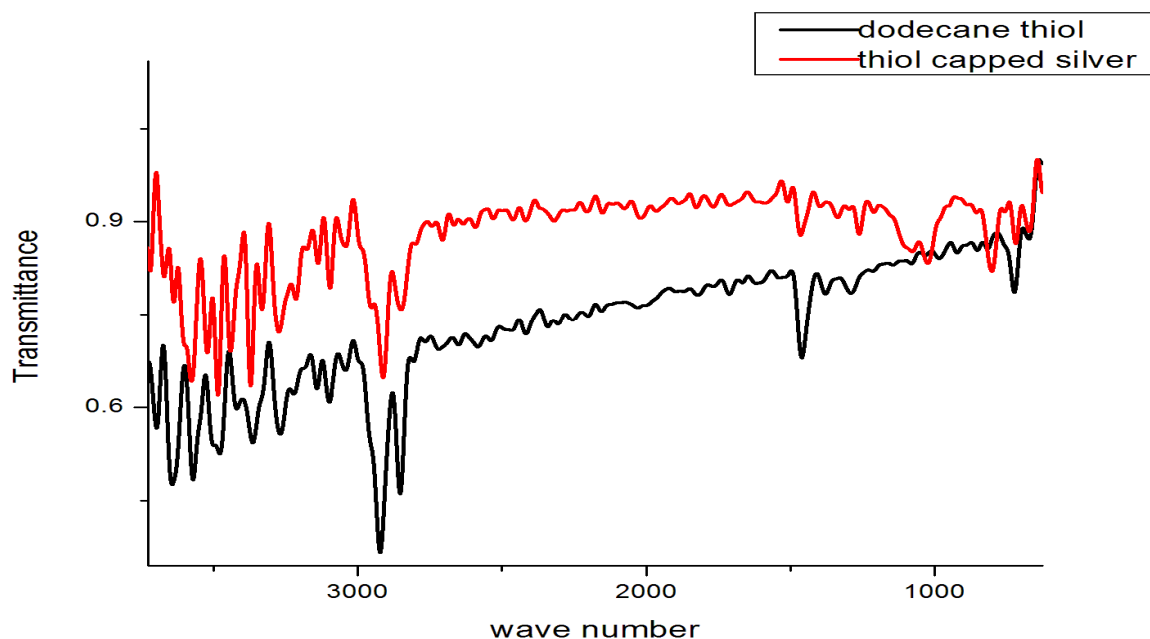


Fig.-6: FTIR of Thiol-capped Ag nanoparticles

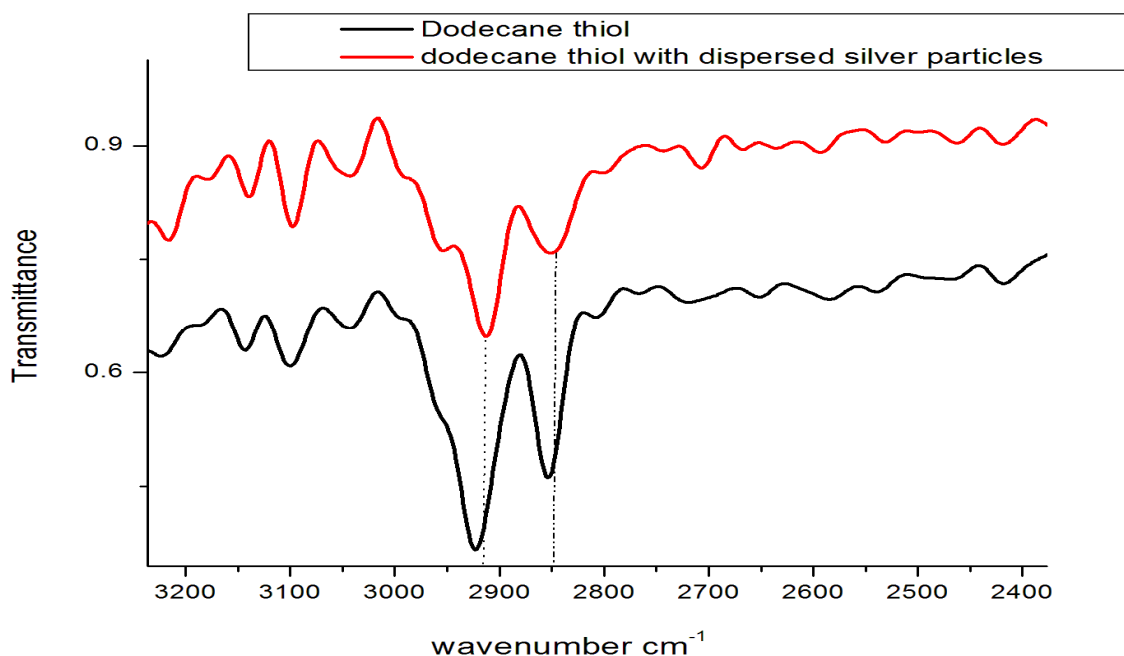


Fig.-7: FTIR showing shift in wavenumber with dispersion of thiol-capped Ag nanoparticles

From the Fig.-7 the asymmetric and symmetric stretching modes clearly appear at 2925.98 and 2857.35 cm^{-1} and these bands shift to lower wavenumber from 2925.98 and 2857.35 cm^{-1} to 2915.15 and 2847.71 cm^{-1} , due to crystallization of thiol-capped Ag nanoparticles, suggesting that Ag nanoparticles are successfully functionalized with dodecanethiol⁴⁷.

SEM analysis

The SEM is used for identification of surface morphology, crystallographic information; grain size and shape of the material. The SEM images of 10OBA with the dispersion of 1wt% thiol-capped Ag nanoparticles are shown in Fig.-9.

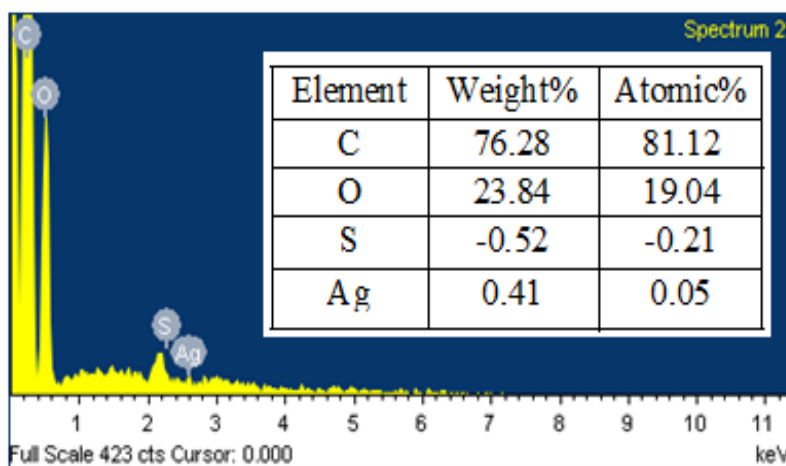


Fig.-8: EDS data of 10OBA with dispersed thiol-capped Ag Nanoparticles

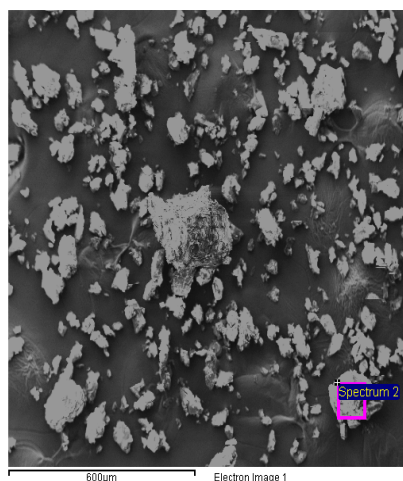


Fig. 9: SEM Image

Results from the energy dispersive spectroscopy (EDS) reveal the presence of chemical compounds in the sample. Carbon (C), Sulphur (S), Silver (Ag) and oxygen (O) elements are present in the 10OBA with dispersed thiol-capped Ag Nanoparticle sample. From EDS data, the presence of nanoparticles in the compound is well established.

XRD Analysis:

XRD data of 10OBA with 1wt% of thiol-capped Ag nanoparticles is shown in Fig.-10. In a comparison of JCPDF data, peaks were well resolved and are matched with JCPDF card No: 040-1471 which is clearly evidenced the existence of thiol-capped Ag nanoparticles in 10OBA. By using Scherrer's Formula, $t = k\lambda / \beta \cos\theta$, grain size of 91 nm is evaluated, where $\Lambda = 1.54 \text{ \AA}$, $\beta = \text{FWHM}$. Peaks at 22.19° , 30.44° and 32.35° also resemble the existence of thiol-capped Ag nanoparticles dispersed in 10OBA.

Optical Birefringence Studies

The Optical Birefringence of 10OBA pure and 10OBA with 1 wt% thiol-capped Ag nanoparticles dispersion were measured by using wedge-shaped cell modified spectrometer having temperature accuracy $\pm 0.1^\circ\text{C}$. The isotropic value splits into higher and lower regions at I-N phase transition which corresponds to extra-ordinary (n_e) and ordinary (n_o) refractive indices. The orientation order parameters n_e and n_o were measured at wavelength 589.3nm. An increment of isotropic phase (n_e) is observed and (n_o) decreases with the decrease of temperature, which is clearly observed at the angle of minimum deviation. Fig.-11 and Fig.-12 represent the variation of refractive indices in 10OBA and 10OBA with 1 wt% thiol-capped Ag nanoparticles. It is found that I-N transition temperature decreased with nanoparticles dispersion which is shown in the DSC and POM values. Further, the birefringence values obtained for 10OBA is nearly equal with the previous results. Birefringence property and its dependency on molecular reorientation play an important role in understanding the molecular reorientation mechanisms^{48,49}. It is

further found that the birefringence anisotropy, $\delta n = n_e - n_o$ value with respect to temperature increases by 22 % with the dispersion of thiol-capped Ag nanoparticles as shown in Fig.-13. It resembles the self-alignment of nanoparticles with 10OBA molecules and thereby the view angle increases which will be very much useful in display devices.

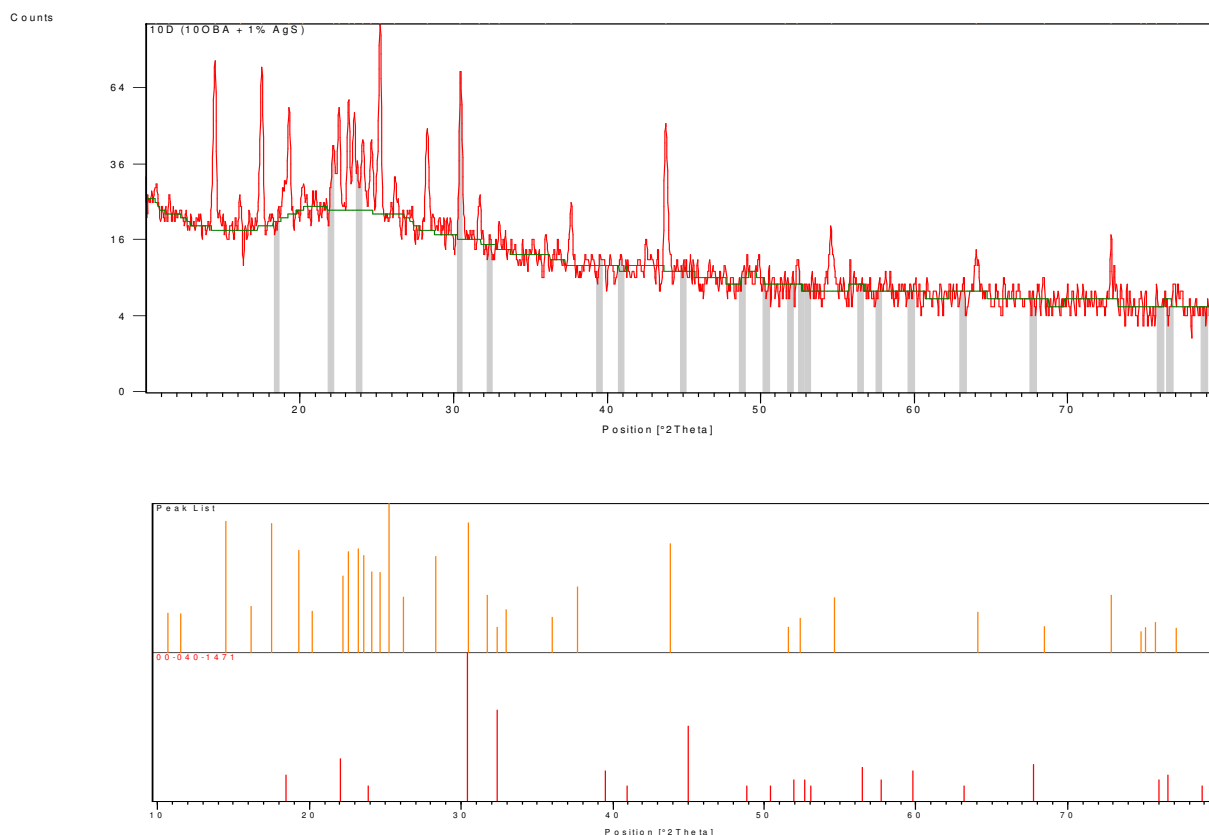


Fig.-10: XRD of 10OBA with dispersed 1wt% of thiol capped Ag nanopartic

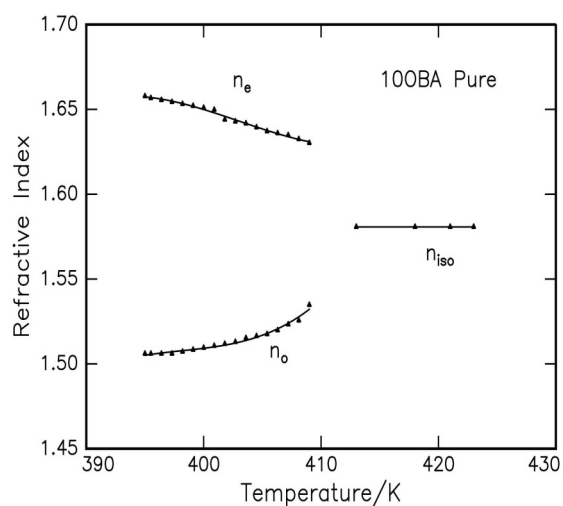


Fig.-11: Refractive index of 10OBA pure

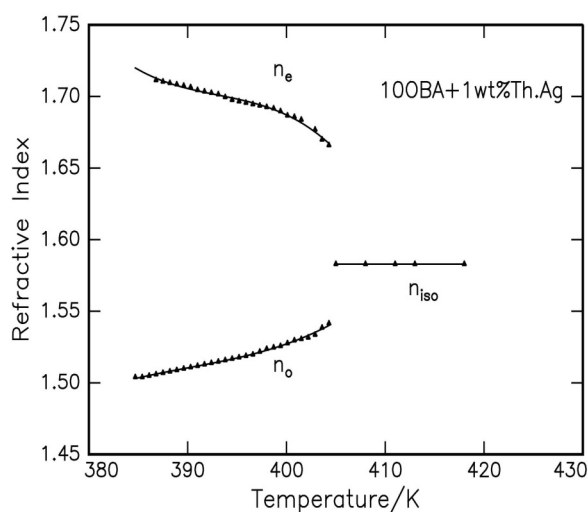


Fig.-12: Refractive index of 10OBA +1 wt% Thiol-capped Ag Nanoparticles

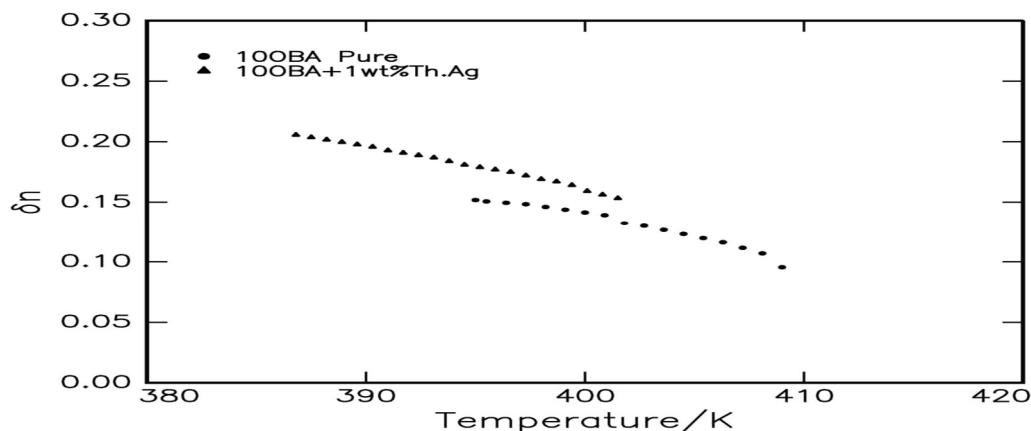


Fig.-13: Variation of δn with temperature in 10OBA Pure and 10OBA with 1 wt% Ag nanoparticle dispersion

CONCLUSION

With the present results we demonstrated the dispersion of thiol-capped Ag nanoparticles in LC 10OBA changing of their textures, phase transition temperatures and shifts in vibrational bands by using Polarizing Microscope, Differential Scanning Calorimeter and Fourier Transform Infra Red techniques respectively. The transition temperatures obtained from polarizing microscope are in good agreement with those obtained from DSC. The transition temperatures of nematic and smectic c phases have reduced while dispersing the thiol-capped Ag nanoparticles. The presence of thiol-capped Ag nanoparticles in LC 10OBA is also confirmed by the EDS data of SEM and UV spectroscopy. X-Ray diffraction confirms no alteration of its structure and also the existence of thiol-capped Ag nanoparticles. X-ray diffraction data also confirms the existence of thiol-capped Ag nanoparticles without altering the host's structure with a grain size of 90nm. With the dispersion of thiol-capped Ag nanoparticles, the birefringence anisotropy of LC compound 10OBA increases by 22 % which will be very much useful for different display techniques.

ACKNOWLEDGEMENT

The author Dr R.K.N.R. Manepalli (Dr M. Ramakrishna Nanchara Rao) is thankful to UGC for grant 42-784/2013 (SR).

REFERENCES

1. H.H. Liang and J.Y. Lee, J.-Y., In *Ferroelectrics – Material Aspects* (ed.Lallart, M.), InTech Publisher, Croatia (2011).
2. S. T. Wu and D. K. Yang, *Reflective Liquid Crystal Displays*, Wiley, New York (2001).
3. C. Tschierske, *Chem. Soc. Rev.*, **36**, 1930 (2007).
4. M. Warenghem, J.F. Henninot and G. Abbate, *Opt. Express*, **2**, 483 (1998).
5. M. Peccianti and G. Assanto, *Opt. Lett.*, **26**, 1690 (2001)
6. J.P.F. Lagerwall and G. Scalia, *J. Mater. Chem.*, **18**, 2890 (2008).
7. W. Lee, C.Y. Wang and Y.C. Shih, *Appl. Phys. Lett.*, **85**, 513 (2004).
8. C.W. Lee and W.P. Shih, *Mater. Lett.*, **64**, 466 (2010).
9. B. Hari Krishna and K. Sandeep Kumar, *Chem. Soc. Rev.*, **40**, 306 (2011).
10. C.M. Jones and E.M.V. Hoek, *J. Nanopart. Res.*, **12**, 1531 (2010).
11. N. Pradhan, A. Pal and T. Pal, *Coll. Sur. A*, **196**, 247 (2002).
12. P.C. Lee and D. Meisel, *J. Phys. Chem.*, **86**, 3391 (1982).
13. L. Shang and S. Dong, *Biosens. Bioelectron.*, **24**, 1569 (2009).
14. S. Chen, H. Gao, W. Shen, C. Lu and Q. Yuan, *Sens. Actuat. B*, **190**, 673 (2014).

15. J. Zhu, X. Song, L. Gao, Z. Li and Z. Liu, S. Ding, S. Zou and Y. He, *Biosens. Bioelectron.*, **53**, 71 (2014).
16. J. Sivasri, M.C. Rao, G. Giridhar, B.T.P. Madav, T.E. Divakar, R. K.N.R. Manepalli, *Rasayan J. Chem.*, **9(4)**, 556 (2016).
17. P. Jayaprada, 588 M. Tejaswi, G. Giridhar, M.C. Rao, V.G.K.M. Pisipati, R.K.N.R. Manepalli, *Rasayan J. Chem.*, **9(4)**, 588 (2016).
18. M. Tejaswi, **M.C. Rao**, P.V. Datta Prasad, G. Giridhar, V.G.K.M. Pisipati, R.K.N.R. Manepalli, *Rasayan J. Chem.*, **9(4)**, 697 (2016).
19. M.C. Rao, O.M. Hussain, *J. Alloys Compd.*, **491(1)**, 503 (2010).
20. M.C. Rao, *J. Crys. Growth*, **312(19)**, 2799 (2010).
21. K. Ravindranadh, M.C. Rao and R.V.S.S.N. Ravikumar, *J. Luminesce.*, **159**, 119 (2015).
22. M.C. Rao, K. Ramachandra Rao, *Int. J. Chem. Tech Res.*, **6(7)**, 3931 (2014).
23. M.C. Rao, *Optoelect. & Adv. Mater. (Rapid Commu.)*, **5**, 85 (2011).
24. Sk. Muntaz Begum, M.C. Rao and R.V.S.S.N. Ravikumar, *Spectrochim. Acta Part A: Mol. & Biomol. Spec.*, **98**, 100 (2012).
25. M.C. Rao, *J. Optoelect. & Adv. Mater.*, **13**, 428 (2011).
26. M.C. Rao, O.M. Hussain, *Eur. Phys. J. Appl. Phys.*, **48(2)**, 20503 (2009).
27. Sk. Muntaz Begum, M.C. Rao and R.V.S.S.N. Ravikumar, *J. Inorg. Organomet. Poly. Mater.*, **23(2)**, 350 (2013).
28. MC Rao, *J. Optoelect. & Adv. Mater.*, **12**, 2433 (2010).
29. M.C. Rao, O.M. Hussain, *IOP Conf. Series: Mater. Sci. Eng.*, **2**, 012037, (2009).
30. M.C. Rao, O. M. Hussain, *Ind. J. Eng. Mater. Sci.*, **16**, 335 (2009).
31. K. Ravindranadh, M.C. Rao, R.V.S.S.N. Ravikumar, *J. Mater. Sci: Mater. Elect.*, **26**, 6667 (2015).
32. M.C. Rao, *Optoelect. & Adv. Mater. (Rapid Commu.)*, **5(5-6)**, 651 (2011).
33. M.C. Rao, O.M. Hussain, *Optoelect. & Adv. Mater.*, **13(2-4)**, 1109 (2011).
34. MC Rao, *J. Optoelect. Adv. Mater.*, **13(1-2)**, 72 (2011).
35. K. Ravindranadh, B. Babu, C.V. Reddy, J. Shim, M.C. Rao, R. Ravikumar, *Appl. Mag. Reson.* **46 (1)**, 1 (2015).
36. MC Rao, OM Hussain, *Res. J. Chem. Sci.*, **1(7)**, 92 (2011).
37. M.C. Rao, *Int. J. Chem. Sci.*, **10(2)**, 1111 (2012).
38. M.C. Rao, *Optoelect. & Adv. Mater. (Rapid Commu.)*, **6**, 511 (2012).
39. P.V. Prasad, K. Ramachandra Rao, M.C. Rao, *J. Mol. Struc.*, **1085**, 115 (2015).
40. M.C. Rao, *J. Optoelect. & Adv. Mater.*, **13**, 78 (2011).
41. M.C. Rao, Sk. Muntaz Begum, *Optoelect. & Adv. Mater. (Rapid Commu.)*, **6**, 508 (2012).
42. MC Rao, *Res. J. Rec. Sci.*, **2(3)**, 67 (2013).
43. A. A. Ledier, B. Tremblay, A. Courty, *Langmuir*, **29**, 13140 (2013).
44. G.W. Gray, *Molecular structures and properties of liquid crystals*, Academic press (1962).
45. A. Ulman, *Chem. Rev.*, **96**, 1533 (1996).
46. J.C. Love, L.A. Estroff, J.K. Kriebel, R.G. Nuzzo and G.M. Whitesides, *Chem. Rev.*, **105**, 1103 (2005).
47. S.C. Park, B.J. Kim, C.J. Hawker, E.J. Kramer, J. Bang and J.S. Ha, *Macromolecules*, **40**, 8119 (2007).
48. M. Ramakrishna Nanchara Rao, P.V. Datta Prasad and V.G.K.M. Pisipati, *Mol. Cryst. Liq. Cryst.*, **528**, 49 (2010).
49. S.T. Wu, *Phys. Rev. A*, **33**, 1270 (1986).

[RJC-1539/2016]